TERRESTRIAL AND MARINE SNOW RESEARCH IN THE NOAA PSL BOUNDARY LAYER DIVISION

David Clemens-Sewall, Brian Butterworth, Christopher J. Cox, Michael Gallagher, Janet Intrieri, Sergey Matrosov, Ola Persson, Matthew Shupe, Anne Sledd

SUMMARY

The Boundary Layer Observations and Processes Division focuses on advancing the understanding of atmospheric boundary-layer processes to promote improved prediction, modeling, and analysis of weather, climate, sea ice and snow, clouds and precipitation, air-sea interactions, and hydrology. We work to build process-level understanding and improve model parameterizations of the snow mass budget and surface energy balance. Our snow mass balance work includes field-based observations of precipitation (e.g., Figure 1), snow loss from sea ice into open water leads (e.g., Figure 2), wind-driven snow redistribution (e.g., Figure 3), and melt processes (not shown). Our surface energy balance work includes autonomous measurements of surface fluxes (Figure 4), spatially-resolved ground-based albedo measurements (not shown), estimates of snow thermal conductivity (e.g., Figure 5), and the representation of these processes in snow and sea ice models (e.g., Figure 6).

PRECIPITATION

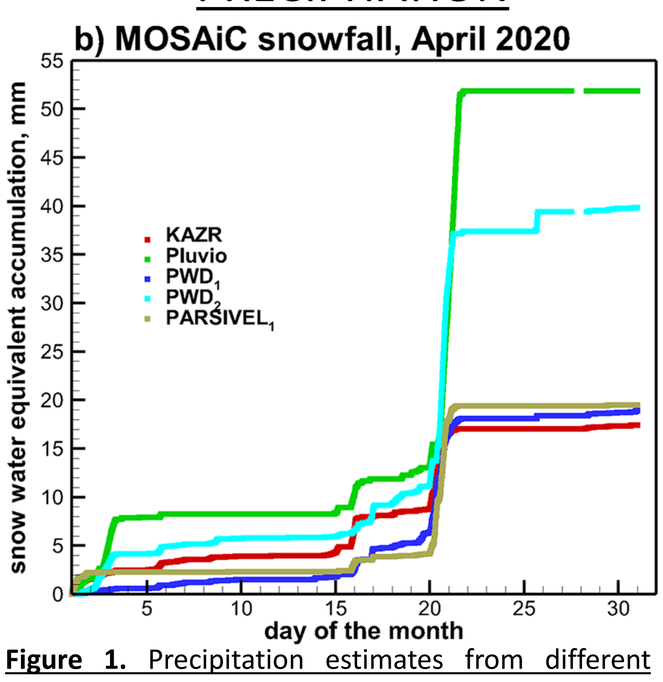

Figure 1. Precipitation estimates from different sensors at the MOSAiC Expedition located on the R/V Polarstern (KAZR, PWD_1, PARSIVEL) and on the ice (Pluvio, PWD_2) (Matrosov et al., 2022). KAZR: Ka-band zenith-pointing radar. Pluvio: weighing bucket precipitation gauge. PWD: Vaisala Present Weather Detectors including optical precipitation gauges. PARSIVEL: Particle Size and Velocity optical disdrometer. Blowing snow effects partially explain the large differences observed between the ice-based and ship-based instruments. Although the ship-based instruments generally agree on the monthly precipitation amount, there are notable differences between the estimated precipitation of individual events.

SNOW LOSS INTO LEADS

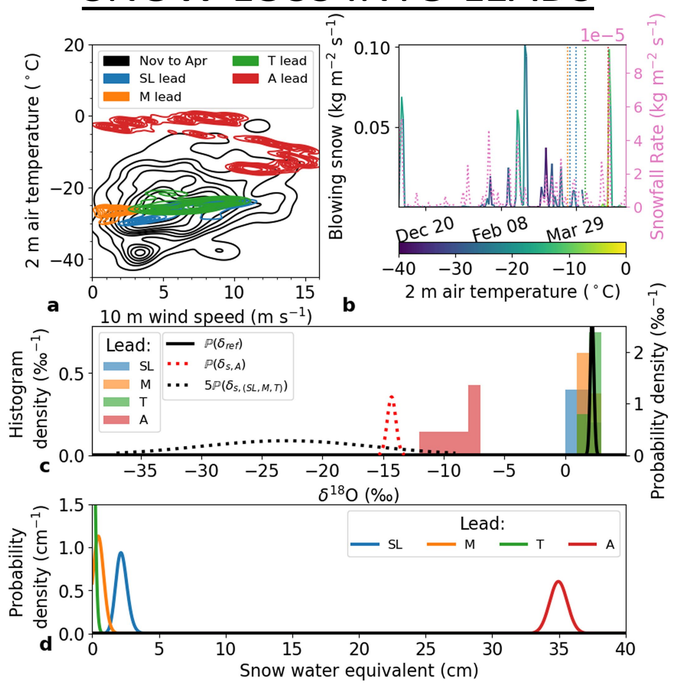

Figure 2. Estimates of wind-blown snow loss into four leads at MOSAiC and concurrent meteorological conditions (Clemens-Sewall et al., 2023). (a) The distribution of 10 m wind speed and 2 m air temperature for November to April at MOSAiC and the distributions at the time of formation for each lead. (b) Blowing snow flux measured nominally 10 cm above the surface, air temperature, and snowfall (Matrosov et al., 2022). Formation dates of leads are indicated by vertical dotted lines (same colors as a, c, d). (c) Histograms $\delta^{18}O$ measurements for each lead and distributions of $\delta^{18}O$ for snow and snow-free ice. (d) Probability distributions of mean snow water equivalent in each lead.

SNOW REDISTRIBUTION

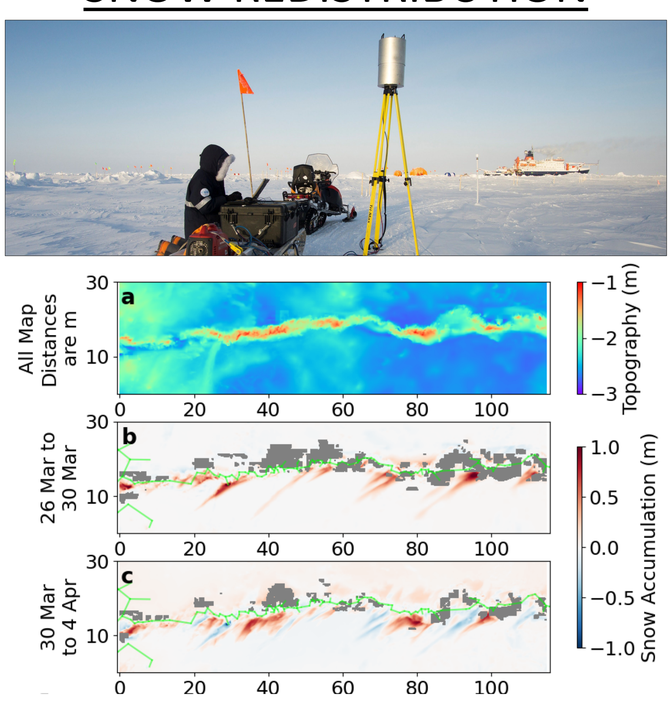

Figure 3. Observations of snow redistribution at MOSAiC via repeat Terrestrial Laser Scanning (TLS) (Clemens-Sewall et al., 2024). (photo) the TLS instrument is mounted on a tripod at various locations to create a topographic map of the snow surface (a). Differencing repeat measurements, aligned into the same, ice-fixed reference frame enables the observation of cumulative snow deposition and erosion (b and c). On Arctic sea ice, snow deposition and erosion is highly spatially variable and concentrated around sea ice pressure ridges (which form aerodynamic obstructions).

SURFACE ENERGY BALANCE

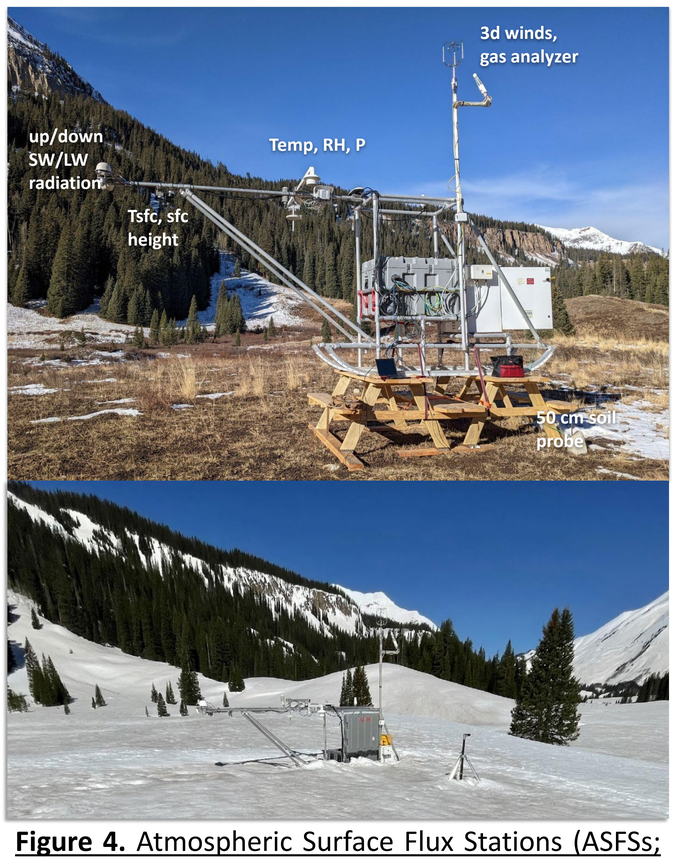

Figure 4. Atmospheric Surface Flux Stations (ASFSs; Cox et al., 2023). Seen here on the SPLASH campaign in Gothic, CO, ASFSs are autonomous packages whose measurements can include: surface meteorology (winds, temperature, pressure, humidity); surface properties (snow-level height, surface IR brightness temperature); energy budget terms (radiative fluxes (LW & SW, up & down), eddy covariance latent & sensible heat fluxes); & soil properties (soil heat flux plates for conductive heat flux, soil moisture (Volumetric Water Content -VWC) & temps at 0-50 cm).

SNOW THERMAL CONDUCTIVITY

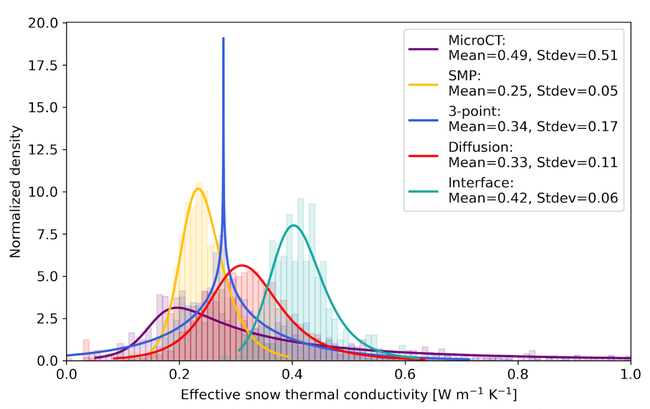

Figure 5. Comparison of estimated effective snow thermal conductivity (ks) at MOSAiC via five different methods (Sledd et al., in prep.). The 3-point (Raphael et al., 2024), Diffusion (Sledd et al., 2024), and Interface (Perovich et al., 2023) methods all use timeseries of vertical temperature profiles recorded by buoys. MicroCT uses finite element modeling of conduction through the ice and air matrix and SMP parameterizes ks as a function of density (using MicroCT), then uses a SnowMicroPen-derived density data set (Macfarlane et al., 2023)

MODELING SNOW IMPACTS

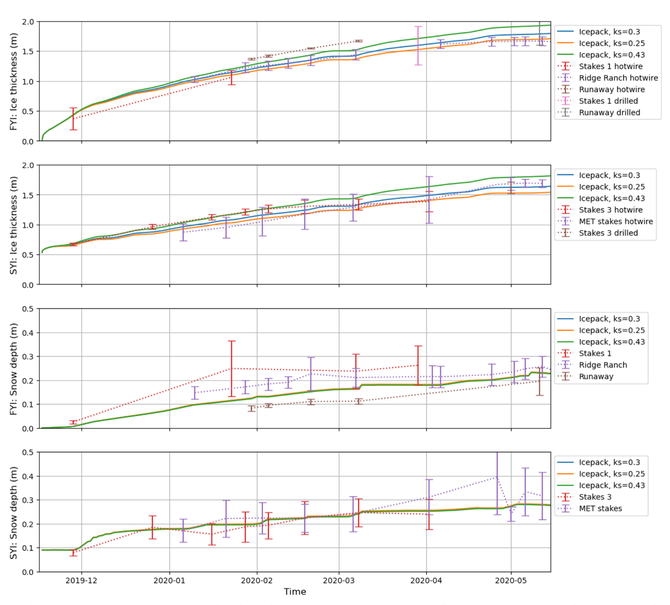

Figure 6. Modeled impacts of snow thermal conductivity (ks) uncertainty (Sledd et al., in prep.). Simulated ice thickness and snow depth evolution for first year ice (FYI) and second year ice (SYI) manual mass balance sites in the MOSAiC Central Observatory (Sledd et al., in prep.). Icepack simulation outputs are shown for three values of ks in solid lines. Observations at manual mass balance sites (Raphael et al., 2024) are shown with dotted lines and errorbars on the dates when measurements were made. Error bars show plus-minus double the standard error of the mean.

REFERENCES

Clemens-Sewall, D., Polashenski, C., Frey, M. M., Cox, C. J., Granskog, M. A., Macfarlane, A. R., et al. (2023). Snow loss into leads in Arctic sea ice: Minimal in typical wintertime conditions, but high during a warm and windy snowfall event. *Geophysical Research Letters*, 50, e2023GL102816. https://doi.org/10.1029/2023GL102816

Clemens-Sewall, D., Polashenski, C., Raphael, I.A. *et al.* High-resolution repeat topography of drifting ice floes in the Arctic Ocean from terrestrial laser scanning. *Sci Data* **11**, 70 (2024). https://doi.org/10.1038/s41597-023-02882-w

Cox, C.J., Gallagher, M.R., Shupe, M.D. *et al.* Continuous observations of the surface energy budget and meteorology over the Arctic sea ice during MOSAiC. *Sci Data* **10**, 519 (2023). https://doi.org/10.1038/s41597-023-02415-5

Macfarlane, A.R., Löwe, H., Gimenes, L., Wagner, D.N., Dadic, R., Ottersberg, R., Hämmerle, S. and Schneebeli, M., 2023. Temporospatial variability of snow's thermal conductivity on Arctic sea ice. *The Cryosphere*, *17*(12), pp.5417-5434.

Sergey Y. Matrosov, Matthew D. Shupe, Taneil Uttal; High temporal resolution estimates of Arctic snowfall rates emphasizing gauge and radar-based retrievals from the MOSAiC expedition. *Elementa: Science of the Anthropocene* 4 January 2022; 10 (1): 00101. doi: https://doi.org/10.1525/elementa.2021.00101

Don Perovich, Ian Raphael, Ryleigh Moore, David Clemens-Sewall, Ruibo Lei, Anne Sledd, Chris Polashenski; Sea ice heat and mass balance measurements from four autonomous buoys during the MOSAiC drift campaign. *Elementa: Science of the Anthropocene* 5 January 2023; 11 (1): 00017. doi: https://doi.org/10.1525/elementa.2023.00017

Ian A. Raphael, Donald K. Perovich, Christopher M. Polashenski, David Clemens-Sewall, Polona Itkin, Ruibo Lei, Marcel Nicolaus, Julia Regnery, Madison M. Smith, Melinda Webster, Matthias Jaggi; Sea ice mass balance during the MOSAiC drift experiment: Results from manual ice and snow thickness gauges. *Elementa: Science of the Anthropocene* 12 January 2024; 12 (1): 00040. doi: https://doi.org/10.1525/elementa.2023.00040

Anne Sledd, Matthew D. Shupe, Amy Solomon, Christopher J. Cox, Donald Perovich, Ruibo Lei; Snow thermal conductivity and conductive flux in the Central Arctic: Estimates from observations and implications for models. *Elementa: Science of the Anthropocene* 12 January 2024; 12 (1): 00086. doi: https://doi.org/10.1525/elementa.2023.00086